Molecular Ordering and Dynamics in the Columnar Mesophase of a New Dimeric Discotic Liquid Crystal As Studied by X-ray Diffraction and Deuterium NMR

S. Zamir,[†] R. Poupko,[†] Z. Luz,*[,†] B. Hüser,[‡] C. Boeffel,[‡] and H. Zimmermann[§]

Contribution from the Weizmann Institute of Science, 76100 Rehovot, Israel, Max-Planck-Institute für Polymerforschung, 6500 Mainz, Germany, and Max-Planck-Institute für Medizinische Forschung, AG Molekülkirstalle, D-6900 Heidelberg, Germany

Received September 7, 1993[⊕]

Abstract: The preparation and mesomorphic properties of a new discotic dimer, bis[pentakis(pentyloxy)triphenylenyloxy]-decane (DTHE5) is described. This molecule is a perfect twin of the monomeric hexakis(pentyloxy)triphenylene (THE5) in that both the spacer and the free alkyl chains are linked via ether bonds and the spacer is exactly twice the length of the free side chains. DTHE5 exhibits a columnar discotic phase which is completely miscible with that of THE5 and is thus classified as D_A, i.e. ordered hexagonal (D_{ho}). X-ray diffraction measurements confirm the assignment and provide geometrical lattice parameters ($a = 20.2$ Å; stacking distance of $d = 3.48$ Å at room temperature) as well as correlation lengths for both (345 and 125 Å, respectively). Deuterium NMR measurements of specifically deuterated DTHE5 in the mesophase region exhibit dynamic line shapes consistent with restricted, high-amplitude, planar librations of the monomeric subunits within the columns. A theory which considers the effect of this motion on the NMR line shape in terms of a diffusion equation in a restricting potential is developed and used to simulate the experimental spectra. The results of the analysis provide kinetic and model related parameters.

Introduction

Discotic liquid crystals usually exhibit columnar phases in which the molecules are stacked into rod-shaped aggregates that in turn are arranged in two-dimensional arrays of various symmetries.[1-3] Typical examples of discogenic molecules are symmetrically substituted benzene,[4] triphenylene,[5] truxene,[6] tribenzocyclononene,[7] and various cyclophanes[8,9] linked via ester or ether bonds to normal alkyl chains. However compounds with lower symmetry are also known to be discogenic, e.g. derivatives of anthracene[10] and of benzopyranobenzopyrandione.[11] More recently synthetic methods were developed which allowed dimerization and polymerization of some of these monomeric discotic liquid crystals. These include dimers of benzene,[12] triphenylene,[13-17] and orthocyclophane[18] linked via spacers of roughly twice the length of the free side chain. A special type of dimer is the "Wheel of Mainz" in which the spacer consists of a stiff aromatic rod.[19] Usually, discotic dimers exhibit similar mesophases as the corresponding monomers, but their range of stability is larger in particular when short spacers are used. Polymerization increases even more the range of the mesophase stability. It was also found that formation of charge transfer complexes with suitable acceptors (trinitrofluorenone derivatives) stabilizes the mesomorphic state of discotic liquid crystals even more.[20-22]

Because of synthetic convenience the spacers used for the dimer formation were linked via ester bonds to the monomeric cores while the free side chains are mostly linked via ether bridges. In the present work we describe the preparation and properties of what may be termed a "perfect twin", bis[pentakis(pentyloxy)-triphenylenyloxy]decane (DTHE5), in which both the free side chains and the spacer are linked to the core by ether bonds and the spacer length is exactly twice that of the free chain. The compound exhibits a mesophase similar to that of the corresponding monomer (hexakis(pentyloxy)triphenylene, THE5), although its range of stability is somewhat larger. Besides the determination of the mesophase structure by X-ray and miscibility measurements our main concern in this paper involves deuterium

† Weizmann Institute of Science.
‡ Max-Planck-Institute für Polymerforschung.
§ Max-Planck-Institute für Medizinische Forschung.
⊕ Abstract published in *Advance ACS Abstracts*, February 1, 1994.

(1) Billard, J. In *Liquid Crystals of One and Two Dimensional Order*; Helfrich, W., Heppke, G., Eds.; Springer-Verlag: New York, 1980.
(2) Levelut, A. M. *J. Chim. Phys. Phys.-Chim. Biol.* **1983**, *80*, 149.
(3) Chandrasekhar, S.; Rangonath, R. S. *Rep. Prog. Phys.* **1990**, *53*, 57.
(4) Chandrasekhar, S.; Sadashiva, B. K.; Suresh, K. A. *Paramana* **1977**, *9*, 471.
(5) Billard, J. B.; Dubois, J. C.; Nguyen, N. T.; Zann, A. *Nouv. J. Chim.* **1978**, *2*, 535.
(6) Destrade, H.; Gasparoux, H.; Babeau, H.; Tinh, N. H. *Mol. Cryst. Liq. Cryst.* **1981**, *67*, 37.
(7) Zimmermann, H.; Poupko, R.; Luz, Z.; Billard, J. *Z. Naturforsch.* **1985**, *40a*, 149. Malthete, J.; Collet, A. *Nouv. J. Chim.* **1985**, *9*, 151.
(8) Zimmermann, H.; Poupko, R.; Luz, Z.; Billard, J. *Liq. Cryst.* **1989**, *6*, 151. Spielberg, N.; Sarkar, M.; Luz, Z.; Poupko, R.; Billard, J.; Zimmermann, H. *Liq. Cryst.* **1993**, *15*, 311.
(9) Bonsignore, S.; Cometti, G.; Dalcanale, E.; du Vosel, A. *Liq. Cryst.* **1990**, *8*, 639. Dalcanale, E.; du Vosel, A.; Levelut, A. M. *J. Chem. Soc., Commun.* **1990**, *63*; *Liq. Cryst.* **1990**, *11*, 93.
(10) Queguiner, A.; Zann, A.; Dubois, J. C.; Billard, J. In *Proceedings of the International Conference on Liquid Crystals. Bangalore*; Heyden and Son: London, 1980; p 35.
(11) Zimmermann, H.; Billard, J.; Gutman, H.; Wachtel, E. J.; Poupko, R.; Luz, Z. *Liq. Cryst.* **1992**, *12*, 245.
(12) Lillya, C. P.; Murthy, Y. L. N. *Mol. Cryst. Liq. Cryst. Lett.* **1985**, *2*, 121.
(13) Kreuder, W.; Ringsdorf, H. *Makromol. Chem. Rapid Commun.* **1983**, *4*, 807.
(14) Kreuder, W.; Ringsdorf, H.; Tschirner, T. *Makromol. Chem. Rapid Commun.* **1985**, *6*, 367.
(15) Wenz, G. *Makromol. Chem. Rapid Commun.* **1985**, *6*, 577.
(16) Werth, M.; Spiess, H. W. *Makromol. Chem. Rapid Commun.* **1993**, *14*, 329.
(17) Kranig, W.; Hüser, B.; Spiess, H. W.; Kreuder, W.; Ringsdorf, H.; Zimmermann, H. *Adv. Mater.* **1990**, *2*, 36.
(18) Percec, V.; Cho, C. G.; Pygh, C.; Tomazos, D. *Macromolecules* **1992**, *25*, 1164.
(19) Kreuder, W.; Ringsdorf, H.; Hermann-Schonherr, O.; Wendorff, J. W. *Angew. Chem., Int. Ed. Engl.* **1987**, *26*, 1249.
(20) Ringsdorf, H.; Wüstefeld, R.; Zerta, E.; Ebert, M.; Wendorff, J. H. *Angew. Chem., Int. Ed. Engl.* **1989**, *28*, 914.
(21) Bengs, H.; Ebert, M.; Karthaus, O.; Kohne, B.; Praefcke, K.; Ringsforf, H.; Wendorff, J. H.; Wüstefeld, R. *Adv. Mater.* **1990**, *2*, 141.
(22) Kranig, W.; Boeffel, C.; Spiess, H. W.; Karthaus, O.; Ringsdorff, H.; Wüstefeld, R. *Liq. Cryst.* **1990**, *8*, 375.

0002-7863/94/1516-1973$04.50/0

Scheme 1. Synthetic Procedure Used To Prepare DTHE5

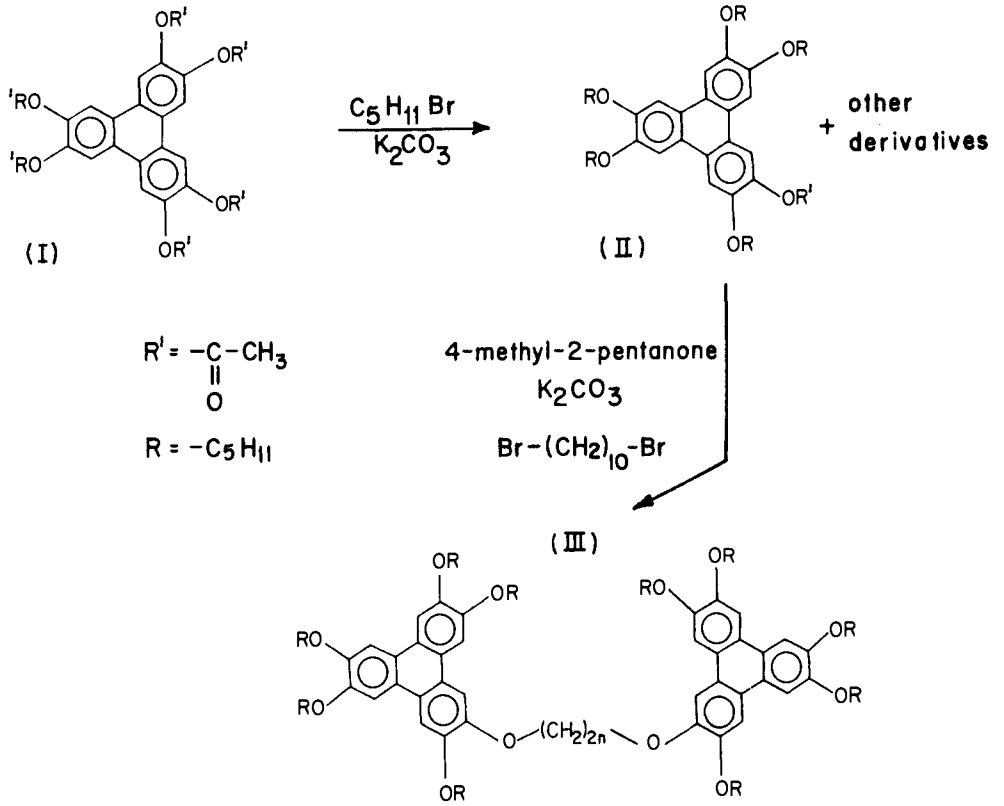

NMR measurements of the mesophase and their interpretation in terms of the motional modes of the molecules within the columns.

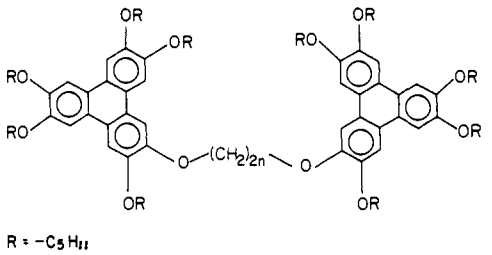

In columnar phases of monomeric discotic liquid crystals there is in general no lateral correlation between the molecules in neighboring columns; the columns can freely slide relative to each other and the molecules randomly reorient about the columnar axes. In low molecular weight discotics the reorientation rate is usually much faster than the overall width of the deuterium NMR spectrum and can therefore not be studied by line shape analysis.[23] Exceptions are some pyramidic liquid crystals, where molecular reorientation is somewhat hindered by the shape of the core,[24,25] and high molecular weight discotics, where reorientation is hindered by the size of the molecules. In the columnar phases of dimeric discotics, correlation is imposed[26,27] by the spacers that link the monomeric units (see Figure 1). If the two subunits of a dimer reside in the same column they can undergo, as a pair, complete reorientation, while if they occupy neighboring columns

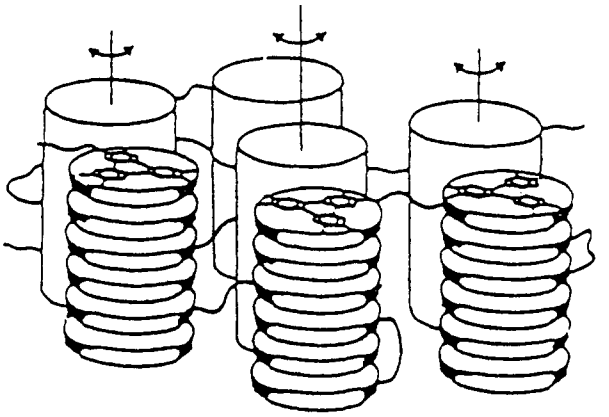

Figure 1. Schematic representation of dimeric discotic molecules in a columnar phase. Note the two possible types of links between the monomeric subunits by the spacer: intracolumnar and intercolumnar.

their freedom to reorient is restricted by the effect of the spacer. The main purpose of the present paper is to characterize the modes of motion in the DTHE5 mesophase, using deuterium NMR spectroscopy. We show that the results can well be interpreted in terms of high-amplitude lateral librations as would be expected from the restriction effect of the spacer if the two dimeric subunits were occupying two neighboring columns.

Experimental Section

(a) Synthesis. The starting material for the preparation of the target compound 1,10-bis[3,6,7,10,11-pentakis(pentyloxy)triphenylenyloxy]-decane (III) was 2-acetyloxy-3,6,7,10,11-pentakis(pentyloxy)triphenylene (II) which was prepared from the corresponding hexakis(acetyloxy) derivative (I) as described in ref 13. II was alkylated (see Scheme 1) with 0.5 equiv of 1,10-dibromodecane in 4-methyl-2-pentanone/K_2CO_3 at 160 °C. After the solvent was removed by low-pressure distillation the residue was crystallized twice from ethanol and the resulting DTHE5 dimer was purified by column chromatography (silica, cyclohexane/CH_2Cl_2 = 3:7) followed by a third recrystallization. Three deuterated species of the

(23) Luz, Z.; Goldfarb, D.; Zimmermann, H. In *Nuclear Magnetic Resonance of Liquid Crystals*; Emsley, J. W., Ed.; D. Riedel Publishing Co.: Dordrecht, 1985.
(24) Poupko, R.; Luz, Z.; Spielberg, N.; Zimmermann, H. *J. Am. Chem. Soc.* **1989**, *111*, 6094.
(25) Zamir, S.; Luz, Z.; Poupko, R.; Alexander, S.; Zimmermann, H. *J. Chem. Phys.* **1991**, *94*, 5927.
(26) Kranig, W.; Boeffel, C.; Spiess, H. W. *Macromolecules* **1990**, *23*, 4061.
(27) Hirschinger, J.; Kranig, W.; Spiess, H. W. *Colloid Polym. Sci.* **1991**, *269*, 993.

dimer were prepared[28] for deuterium NMR measurements, including DTHE5 deuterated in the unsubstituted aromatic sites, in the α-methylenes of the pentyloxy side chains, and in the α-methylenes of the spacer. The aromatic deuterated isotopomer was prepared from the isotopically normal compound by exchange with a large excess of CF_3COOD under reflux for 24 h, followed by distillation for removing the trifluoroacetic acid and purification as described above, using ethanol-*d* in the crystallization step. The other two isotopomers were prepared with use of appropriately deuterated starting materials, viz., pentyl-$\alpha,\alpha,-d_2$ bromide and 1,10-dibromodecane-*1,1,10,10-d*$_4$. All products were checked by NMR and mass spectrometry and gave the expected spectra with essentially no traces of impurities.

(b) X-ray Measurements. The θ–θ diffractograms were obtained on a Siemens Kristalloflex diffractometer (35 kV, 30 mA) equipped with a heating stage, using Ni-filtered Cu Kα radiation (λ = 1.5406 Å) in the reflection mode with a 0.3- or 0.15-mm collimator. The sample consisted of a vacuum annealed (140 °C) powder specimen.

(c) NMR Measurements. Deuterium NMR spectra of the various isotopomers were recorded at 46.07 MHz on a high-power Bruker CXP 300 spectrometer equipped with a BVT 1000 variable-temperature unit. The spectra were obtained by the quadrupole echo method, $(\pi/2)_{\pm x}$–τ–$(\pi/2)_y$–τ–(± acquisition) with appropriate phase cycling, followed by Fourier transformation. The $\pi/2$ pulses were between 2 and 3 μs long and the recycle time ranged between 0.5 and 5 s.

Results

(a) Differential Scanning Calorimetry and Polarizing Optical Microscopy. Differential scanning calorimetry thermograms of DTHE5 and THE5 are shown in Figure 2. Both show a similar phase sequence

$$\text{solid} - \text{M} - \text{iso}$$

with essentially identical melting points of 65.0 and 67.0 °C for the monomer and dimer, respectively, but quite different clearing points of 121.0 and 135.6 °C. These results are for heating of crystalline samples, cooling usually results in considerable supercooling of the mesophase. Under optical microscopy the mesophases of the dimer and monomer exhibit similar features typical of uniaxial columnar phases. A contact preparation of THE5 and DTHE5 showed complete miscibility of the two mesophases, indicating the equivalence of their structure. This structure was determined by X-ray studies of the THE5 monomer to be ordered columnar with hexagonal symmetry, i.e., D_A (D_{ho}).[29,30]

(b) X-ray Diffractometry. X-ray diffractograms of the DTHE5 mesophase at 127 °C and in the supercooled state at room temperature (27 °C) are shown in Figure 3. In the large-angle range they exhibit a broad peak at around $2\theta \sim 19°$ (typical for diffraction from disordered alkyl chains[2]) and a somewhat narrower peak at $2\theta \sim 25°$ ($\sim$ 3.5 Å) which is assigned to diffraction from the stacking periodicity of the molecules within the columns. As may be seen, the position and width of the peak are temperature dependent. In the low-angle region a strong narrow peak is observed at 5.06° and a weak one at 13.5°. At very high gain two more extremely weak peaks may barely be detected just above the noise level at 8.9° and 10.2° (their position is indicated by arrows above the room temperature trace). These low-angle peaks can be indexed on a two-dimensional hexagonal lattice as shown in Table 1. The hexagonal lattice parameter, 20.2 Å, is very similar to that found[2] in the mesophase of THE5 (18.95 Å) and is only slightly smaller than the diameter of a stretched all-trans THE5 molecule ($\sim$22 Å). These results indicate that the columns in the DTHE5 mesophase consist of stacked triphenylene units as in the corresponding THE5 monomer (Figure 1). The fact that the column's diameter is smaller than 22 Å reflects the disorder of the alkyl chains and their partial interleaving in the mesophase.

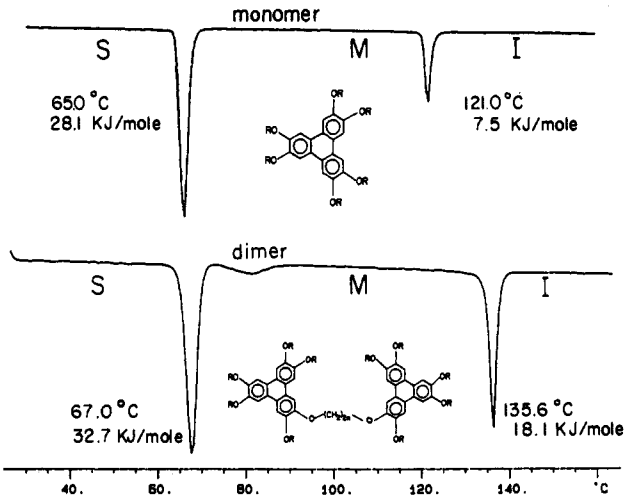

Figure 2. Differential scanning calorimetry thermograms of the monomer THE5 and the dimer DTHE5. The data are for a first heating run (10 °C per min) of a crystallized compound.

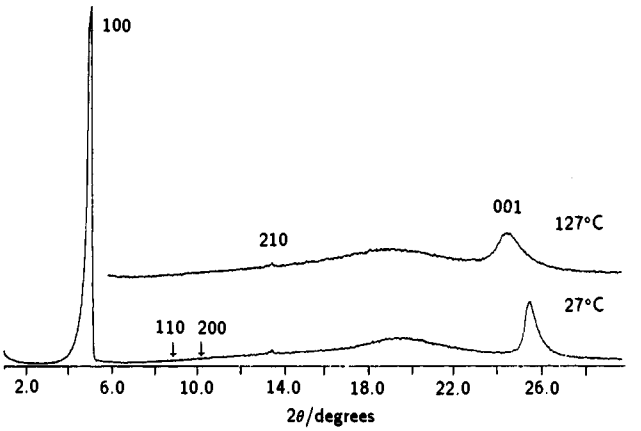

Figure 3. X-ray diffractograms obtained in the discotic mesophase of DTHE5 at room temperature (supercooled) and 127 °C. The Miller indices of the observed peaks are indicated. Two additional diffractions at 2θ = 8.9° and 10.2° (see arrows) can only be observed at much higher gain. The broad band at 2θ = 19° is due to diffraction from the disordered alkyl chains.

Table 1. X-ray Diffractions Observed in the (Supercooled) Mesophase of DTHE5 at 27 °C

2θ (deg)	*d* spacing[a] (Å)	Miller indices (*hkl*)
5.06	17.47	(100)
8.90	9.93	(110)
10.2	8.67	(200)
13.5	6.55	(210)
22.0–19.6	4.04–4.54	alkyl chains
25.8	3.48	(001)

[a] $d = 1.5406/2 \sin \theta$.

The widths of the diffraction peaks provide a measure of the various correlation lengths in the columnar structure. Thus the sharpness of the 100 reflection indicates high order in the hexagonal packing of the columns, while the relatively large width of the 001 peak indicates a comparatively lower order in the stacking of the molecules within the columns. We have measured the X-ray diffraction in the DTHE5 mesophase at several temperatures from room temperature up to close to the clearing point. The results for the 100 and 001 diffraction peaks are summarized in Table 2. They also include the corresponding correlation lengths, ξ, as determined from the equation[31]

$$\xi_{hkl} = 0.9\frac{\lambda}{\Delta\theta_{hkl}\cos\theta_{hkl}}$$

(28) Zimmermann, H. *Liq. Cryst.* **1989**, *4*, 591.
(29) Levelut, A. M. *J. Phys. Lett.* **1979**, *40*, L-81.
(30) Destrade, C.; Gasparoux, H.; Foucher, P.; Tinh, N. H.; Malthete, J.; Jacques, J. *J. Chim. Phys. Phys.-Chim. Biol.* **1983**, *80*, 137.

Table 2. Lattice Parameters and Correlation Lengths in the DTHE5 Mesophase at Various Temperatures

T (°C)	d_{100} (Å)	$\Delta\theta_{100}$ (deg)	ξ_{100} (Å)	ξ_{100}/d_{100}	d_{001} (Å)	$\Delta\theta_{001}$ (deg)	ξ_{001} (Å)	ξ_{001}/d_{001}
27[a]	17.5	0.23	345	20	3.48	0.65	125	36
75	17.6	0.20	395	22	3.54	0.78	100	28
97	17.7	0.22	360	20	3.57	0.90	90	25
127	17.6	0.26	305	17	3.63	1.16	70	19

[a] Supercooled.

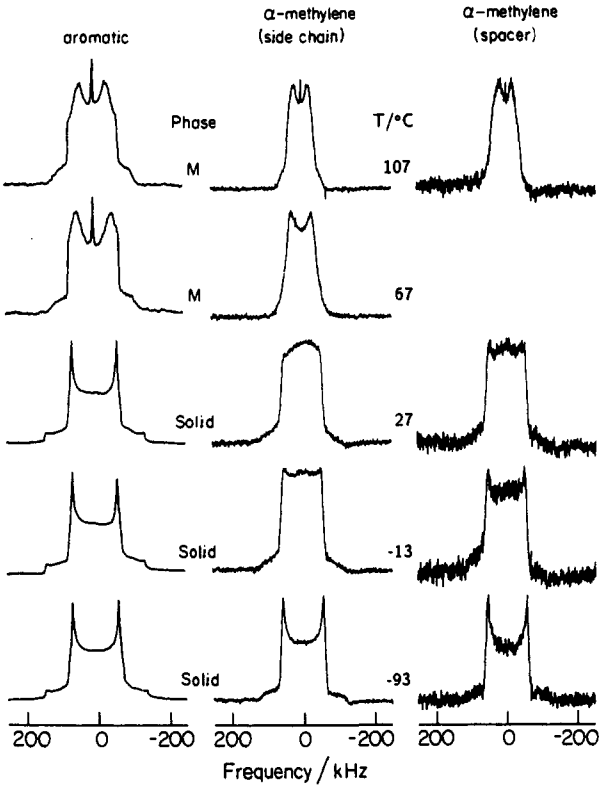

Figure 4. Deuterium NMR spectra of the three different DTHE5 isotopomers in the solid and mesophase regions at the indicated temperatures.

where $\Delta\theta_{hkl}$ is the full width of the peak at half maximum intensity and the coefficient 0.9 is a correction factor which depends on the shape of the domains. For fairly regular shapes it usually varies[31] between 0.8 and 1.0, hence our choice of 0.9. It may be seen that the lattice parameter and the correlation length associated with the 100 peak are almost independent of temperature, with $\xi_{100}/d_{100} \approx 20$, while the corresponding value for the 001 peak is quite sensitive to the temperature; the stacking distance increases by about 4% in the temperature range 27–127 °C, and at the same time ξ_{001}/d_{001} decreases by almost a factor 2 (from 36 to 19). The estimated error in the correlation lengths of the intracolumnar stacking is ±15%, due partly to the experimental error in determining Δ and partly to the uncertainty in the correction coefficient. The trend in ξ_{001} as shown in Table 2 is however quite clear. The correlation lengths are lower than those determined for the THE5 monomer but considerably higher than in nonsymmetrically substituted triphenylenes[32] and thiotriphenylenes.[33]

(c) Deuterium NMR Spectra. Deuterium NMR spectra of powder samples of the three deuterated isotopomers of DTHE5 in the solid and mesophase regions are shown in Figure 4. All spectra were obtained by heating the solid and the temperature was kept well below the clearing point to avoid possible alignment. Under these conditions the shapes of the spectra were reproducible upon cooling and reheating. The spectra of the aromatic deuterons in the solid phase are typical of a rigid system and undergo an abrupt change at the transition to the mesophase. This clearly indicates that the triphenylene moiety is static in the solid while in the mesophase it undergoes some kind of motion. In contrast, the deuterium spectra of the α-methylene groups in both the side chains and the spacer exhibit dynamic behavior already in the solid state. Since the triphenylene core is static in the solid the dynamic effect must be assigned to conformational disorder. At the melting temperature a discontinuous change takes place in the spectrum of the α-methylene groups which no doubt reflects the setting-in of overall molecular motion as is also observed in the aromatic deuterons. We have not analyzed these line shapes quantitatively, but it is noteworthy that in both the solid and the mesophase the signals of the free side chains and of the spacers give very similar patterns.

The main concern of the present work is the analysis of the NMR spectra of the aromatic deuterons in the DTHE5 mesophase. As may be seen in Figure 4, melting of the solid results in a discontinuous change whereby the typical spectrum of a nearly uniaxial quadrupole tensor ($\eta = 0.05$) is transformed to one with a clear biaxial symmetry in which one canonical axis (which we identify as Y_P) remains essentially unchanged relative to its value in the solid. Such behavior is characteristic of a restricted planar reorientation (about Y_P) as would for example be expected if the triphenylene moiety were undergoing two site jumps or restricted librations (in the X_PZ_P plane).[34] This observation immediately indicates that the dimer molecules, or at least most of them, occupy neighboring columns rather than the same column where no such restricted motion is expected (see Figure 1).

With increasing temperature the line shape continues to evolve and the asymmetry parameter gradually increases until the melting point where the spectrum collapses to a single line. The spectra shown in Figure 4 were recorded by the quadrupole echo method using a time interval, $\tau = 20$ μs, between the first two pulses in the sequence. Upon increasing τ the intensity of the spectrum decreases, and at the same time its overall shape changes. Such "echo distortions" reflect T_2 anisotropy due to motional effects and are usually quite sensitive to the mechanisms and rates of dynamic processes.[35] In the next section we present a model for the motion of the triphenylene units in the columnar mesophase and develop a theory for simulating dynamic NMR spectra obtained by quadrupole echo experiments. We then use this theory to analyze the τ-dependent spectra obtained experimentally for the DTHE5 mesophase in order to derive kinetic and model related parameters for the molecular motion.

(d) Dynamic Model and Comparison with Experimental Results. As a first attempt to interpret the results we tried to simulate the spectra using a two-site jump model. However although we could obtain the correct asymmetry parameters, the line shapes and in particular the τ-dependence could not be satisfactorily reproduced. We therefore adopted a model in which each half of the DTHE5 dimer is librating under the effect of a restricting potential due to the spacer. To simplify the calculation we assume that each subunit librates independently by fixing the other end of the spacer at the center of the neighboring column. For a given triphenylene moiety the energy will be minimal when the spacer is least stretched, i.e. when its fixed point (F), the bridging point (B), and the core center (C) lie on a straight line (see Figure 5a). As the core reorients in the plane its potential energy increases and the associated probability decreases in accordance with the

(31) Guinier, A. *X-Ray Diffraction*; W. H. Freeman and Co.: San Francisco, 1963; Chapter 5.
(32) Werth, M.; Valerien, S. U.; Spiess, H. W. *Liq. Cryst.* **1991**, *10*, 759.
(33) Heiney, P. A.; Fortes, E.; de Jeu, W. H.; Riera, A.; Carroll, P.; Smith, A. B., III *J. Phys. (Paris)* **1989**, *50*, 461.
(34) Sparks, S. W.; Budhu, N.; Young, P. E.; Torchia, D. A. *J. Am. Chem. Soc.* **1988**, *110*, 3359. Hirschinger, J.; English, A. D. *J. Magn. Reson.* **1989**, *85*, 542.
(35) Vega, A. J.; Luz, Z. J. *Chem. Phys.* **1987**, *86*, 1803.

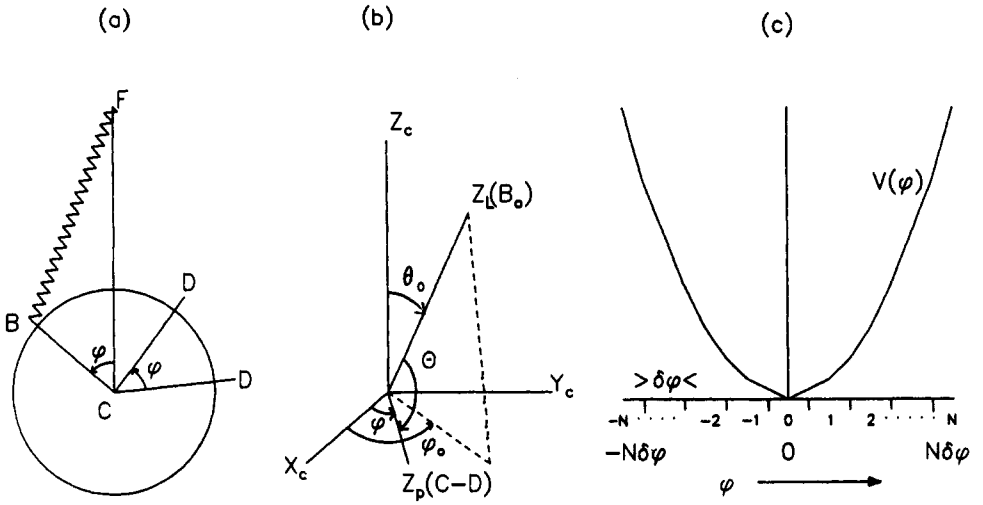

Figure 5. (a) A model for the librational motion of the monomeric subunit under the restriction force of the spacer, assumed to be fixed at point F and linked to the triphenylene moiety at point B. The angle φ is the deflection from equilibrium of the bridging point and also of any aromatic C–D bond. (b) The coordinate systems used in the calculation: X_c, Y_c, Z_c refer to the columns with Z_c along the columns direction, X_cY_c is the plane of libration of the monomeric subunits, Z_p is the direction of the principal quadrupole tensor direction (the C–D bond) and Z_L is the direction of the external magnetic field with polar angles θ_0 and φ_0 in the coordinate system X_c, Y_c, Z_c. (c) A plot of the potential energy $V_0\varphi^2$ as function of φ and the discretization of φ into $2N + 1$ segments.

Boltzman distribution. For concreteness we assume a potential of the form

$$V(\varphi) = V_0\varphi^2 \tag{1}$$

where V_0 is a positive parameter with dimensions energy/rad^2, as for a torsional spring, while φ is the deflection of the CB vector from its equilibrium (minimum energy) direction. Although this potential is very simple minded, it does contain the main features of the assumed model: the energy for right and left deflections is the same, $V(\varphi) = V(-\varphi)$, and a proper choice of the parameter V_0 will restrict the librational amplitude until the desired fit to the experimental results is obtained. In the calculation we assume for each C–D bond a normalized equilibrium distribution

$$P^0(\varphi) = \sqrt{\frac{\beta V_0}{\pi}}\exp(-\beta V_0\varphi^2) \tag{2}$$

where $\beta = (kT)^{-1}$. The librational motion of the core under the restricting effect of the spacer is assumed to obey a diffusion equation for the distribution, $P(\varphi,t)$, of the C–D bonds of the form[36,37]

$$\frac{d}{dt}P(\varphi,t) = \left[D_R\frac{\partial^2}{\partial\varphi^2} + \beta D_R\frac{\partial V(\varphi)}{\partial\varphi}\frac{\partial}{\partial\varphi} + \beta D_R\frac{\partial^2 V(\varphi)}{\partial\varphi^2}\right]\times$$
$$P(\varphi,t) = \Gamma(\varphi)\,P(\varphi,t) \tag{3}$$

where D_R is a reorientational diffusion constant. By using eq 1, $\Gamma(\varphi)$ becomes

$$\Gamma(\varphi) = D_R\frac{\partial^2}{\partial\varphi^2} + \left[2V_0\beta\varphi D_R\frac{\partial}{\partial\varphi} + 2V_0\beta D_R\right] \tag{4}$$

in which the first term corresponds to free self-diffusion and the second to a potential driven diffusion. The corresponding Liouville equation for the complex magnetization $M(\varphi,t) = M_X(\varphi,t) + iM_Y(\varphi,t)$ (in the rotating coordinate system) then becomes

$$\frac{d}{dt}M(\varphi,t) = -im\omega_Q(\Theta)\,M(\varphi,t) - \left(\frac{1}{T_2} - \Gamma(\varphi)\right)M(\varphi,t) \tag{5}$$

where $\omega_Q(\Theta)$ is the quadrupole frequency and is related to the orientation of the C–D bond direction relative to that of the magnetic field

$$\omega_Q(\Theta) = \frac{3}{4}\frac{e^2qQ}{\hbar}\frac{1}{2}[3\sin^2\theta_0\cos^2(\varphi_0-\varphi) - 1 +$$
$$\eta(\cos^2\theta_0 - \sin^2\theta_0\sin^2(\varphi_0-\varphi))] \tag{6}$$

The coordinate system and angles used are defined in Figure 5b: X_c, Y_c, Z_c are the coordinates of a column with Z_c along the column's axis; the molecule is assumed to librate in the X_cY_c plane with X_c the equilibrium direction of the C–D bond; θ_0, φ_0 are the polar and azimuthal angles of the magnetic field B_0; Z_p is the principal quadrupole axis of the deuteron assumed to be along the C–D bond; and Y_p is parallel to Z_c. The coefficient m in eq 6 is +1 for the $m_I = 1$ component of the quadrupole doublet and −1 for the other component. The two subspectra are related by reflection about the zero-frequency point.

In the Appendix we develop a formalism for solving eq 5 where details about the computation procedure are also described. In the following we use this method to simulate spectra which best fit the experimental results. This will allow us to obtain experimental parameters related to the proposed model.

It was indicated in section c that the dynamically averaged asymmetry parameter in the mesophase increased with temperature from $\eta = 0.1$ to 0.3. In our model this reflects an increase in the librational range, partly due to increase of kT in the Boltzman equation and also due to a decrease in the restriction force, V_0, with increasing temperature. To get a feeling for the approximate ranges of φ and V_0 that fit our model we use the two-site jump expression for η. For a jump by 2γ the average tensor components become $q_x = {}^1/_2(3\sin^2\gamma - 1)$, $q_y = -{}^1/_2$, and $q_z = {}^1/_2(3\cos^2\gamma - 1)$ (in units of $(3/4)(e^2qQ/\hbar)$), so that provided 2γ does not exceed 70.6°, η is given by

$$\eta = \frac{q_x - q_y}{q_z} = \frac{3\sin^2\gamma}{3\cos^2\gamma - 1} \tag{7}$$

(36) Freed, J. H. In *Spin Labelling, Theory and Applications*; Berliner, L. J., Ed.; Academic Press: New York, 1976; p 53.
(37) Zamir, S.; Poupko, R.; Luz, Z.; Alexander, S. *J. Chem. Phys.* **1991**, *94*, 5939.

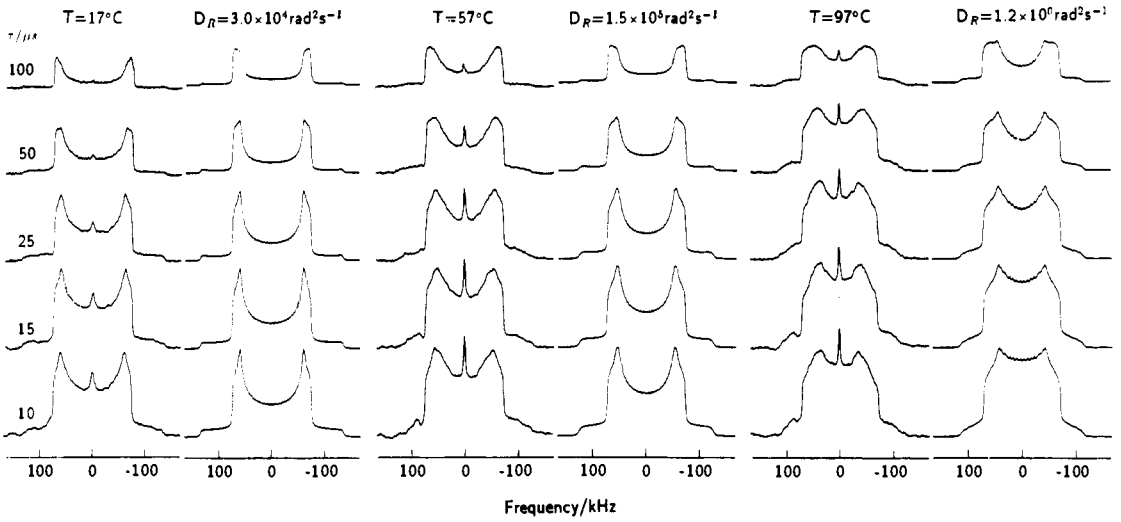

Figure 6. Experimental and simulated deuterium NMR spectra of the aromatic deuterons in the mesophase of DTHE5 at three different temperatures for different values of the pulse delay, τ. For each temperature the intensity of the spectra is normalized to that of the shortest τ (10 μs). The simulated spectra were calculated as described in the text using the values shown in Table 3.

From the experimental results for η this corresponds to γ values ranging from 14° to 23°. An estimate for V_0 can then be obtained by solving the equation

$$\langle|\gamma|\rangle = 2\sqrt{\frac{\beta V_0}{\pi}}\int_0^\infty \varphi \exp(-\beta V_0 \varphi^2)\, d\varphi \qquad (8)$$

yielding $\beta V_0 \sim 3.5$.

To get quantitative information about the diffusion parameter D_R we need to compare the actual line shape with simulated spectra. We found that particularly sensitive to the dynamic parameter was the dependence of the line shape on the time interval, τ, between the $\pi/2$ pulses in the quadrupole echo sequence. Accordingly in the analysis we emphasize the fit to spectra recorded with variable τ. In Figure 6 are shown such spectra for three different temperatures. Most spectra exhibit a relatively sharp center peak of the type that is often observed in deuterium NMR of discotic mesophases. It is usually ascribed to traces of remaining solvent or impurities and will be disregarded in the following discussion. It may be seen that in all cases, increase of τ not only reduces the overall intensity of the NMR signal due to transverse relaxation but also causes characteristic changes in the line shape. We have tried to simulate the spectra by adjusting at each temperature the values for D_R and βV_0. Most details of the spectra could reasonably well be fitted with just these parameters, except that the q_x feature came up much sharper in the simulations than in the experiments. Such an effect could result from a distribution in βV_0, and for the final simulations we have therefore included some distribution in this parameter. The distribution was taken to be Gaussian with $\beta\sigma$ = 2.0 rad^{-2} for all temperatures. In practice 7 to 11 values of βV_0 about the average value were employed for each simulation. Simulated spectra calculated in this way are shown in Figure 6 to the right of the corresponding experimental spectra. The whole set of parameters used in the simulations is summarized in Table 3. The line width and asymmetry parameters were taken to be independent of the temperature, $1/T_2 = 10^3$ s^{-1}, $\eta = 0.05$, but the quadrupole interaction, $(3/4)(e^2qQ/h)$, was slightly changed from its static value (143 kHz) by using an effective temperature dependent order parameter to account for a small degree of orientational disorder in the mesophase.

The simulations shown in Figure 6 are not perfect, in particular they fail to exactly reproduce the center part of the spectra, which in the simulation often has a lower intensity than in the experiments. They do however reproduce pretty well the general features of the experimental results, including the asymmetry parameter, the overall reduction of the signal intensity with τ, and the relative decrease in the intensity at different frequency regions of the spectrum. These features were quite different in spectra simulated for two-site jumps, a mechanism which we therefore rejected in favor of the libration model. An important point of the simulations is their sensitivity not only to V_0 but mainly to D_R which allowed us to obtain dynamic information as summarized in Table 3.

Table 3. Parameters Used in the Simulation of the Experimental NMR Spectra of the Aromatic Deuterons in the Mesophase of DTHE5

T (°C)	βV_0[b] (rad^{-2})	D_R (rad^{-2} s^{-1})	$S(3/4)(e^2qQ/h)$ (kHZ)
17[a]	13.0	3.0×10^4	143
37[a]	9.5	4.0×10^4	142
57[a]	6.8	1.5×10^5	140
77	4.5	4.0×10^5	139
97	2.5	1.2×10^6	135

[a] Supercooled. [b] Average value, with a constant Gaussian distribution of 2.0 rad^{-2} width.

(e) NMR Spectra in Aligned Samples. The spectra discussed in the previous section were all of completely disordered powder samples obtained from the solid by melting. To substantiate the dynamic model used for the interpretation of the results we also recorded spectra of partially aligned samples. It is well-known that discotic columnar phases can be oriented by cooling the liquid to the mesophase while inside a sufficiently strong magnetic field.[38] Since the anisotropic magnetic susceptibility of the triphenylene core is negative the mesophase aligns with the columns (director) perpendicular to the field direction. If the cooling is done while slowly spinning the sample about an axis perpendicular to the field direction, a monodomain sample is obtained with the director parallel to the spinning axis. Once aligned and cooled well below the clearing temperature the orientation will usually stay. We have prepared such a single domain sample of DTHE5 by slowly rotating the sample inside the spectrometer's magnetic field (7.04 T), using a probe equipped with a goniometer. The spectra were then recorded at different temperatures without removing the sample from the probe. The results are shown in Figure 7. These spectra therefore correspond to the magnetic field perpendicular to the director and thus the static component $q_y = -1/2$ of the quadrupole tensor is not observed. The spectrum is typical of a two-dimensional powder with two principal components q_x and q_z. The dynamic process is reflected

(38) Goldfarb, D.; Luz, Z.; Zimmermann, H. *J. Phys.* (*Paris*) **1981**, *42*, 1303.

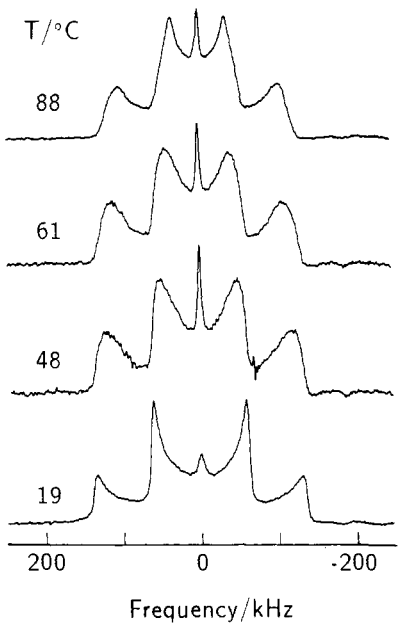

Figure 7. Deuterium NMR spectra of the aromatic deuterons in the mesophase of DTHE5 in an aligned sample with the director perpendicular to the magnetic field. The spectra were recorded at different temperatures as indicated with $\tau = 20$ μs.

in a decrease in the absolute values of q_x and q_z and a corresponding increase in η. Since the trace $q_x + q_y + q_z = 0$, eq 7 becomes $\eta = (2q_x + q_z)/q_z$. Application to the spectra in Figure 7 gives essentially the same η values as those obtained from the powder. We did not however perform a complete line shape analysis and τ-dependence measurements on the aligned sample as we did for the powder. Since the alignment of the sample is not perfect a detailed line shape analysis would require knowledge of the domain distribution which we do not have.

Summary and Discussion

We have shown that in the columnar mesophase of the dimer DTHE5 the monomeric subunits constitute the building elements of the columns in much the same way as in the columnar phases of the discotic monomers. Two possibilities of occupying the columns can be imagined as shown in Figure 1: (i) the two subunits reside in the same column above each other and (ii) the two subunits reside in neighboring columns. In (i) there is no restriction on the angular range that the molecules can span while in (ii) such a restriction is strongly imposed by the spacer. The fact that experimentally we found that the librational motion is strongly restricted indicates that the second alternative is the dominant one for the dimer.

Our analysis yielded kinetic parameters for the restricted reorientational diffusion as well as model related parameters. We find that the angular restriction is quite significant, confining the librational amplitude to between ±13° and ±30° in the temperature range 20–100 °C. The effect of the spacer is described in terms of a torsional spring obeying Hooke's law with a force constant of $\sim 5 \times 10^{-13}$ erg rad^{-2} per molecule, which is very similar to the torsional energies in simple aliphatic bonds. Noticeably the diffusion constant D_R (Table 3) is considerably slower than that for free reorientation in normal monomeric discotic liquid crystals and the corresponding activation energy (13.6 kcal mol^{-1}) is significantly higher than expected for free reorientational diffusion. Apparently the spacer's effect is more than merely to restrict the angular range of the diffusion. Referring to Table 3 we note that V_0 decreases with increasing temperature and, over the experimental range studied, can be fit to the equation

$$V_0 = 27.9 - 0.07T \text{ (kcal mol}^{-1}\text{ rad}^{-2}\text{)}$$

The decrease in the force constant and associated increase in the libration amplitude no doubt reflects the weakening of the lattice forces that keep the "other end" of the spacer in place. As the temperature is further increased we can anticipate intercolumnar jumps of the triphenylene moiety resulting in an effective overall reorientation of each subunit. Such a process is clearly not occurring at a rate sufficiently fast to affect the line shape, but it could perhaps be observed by 2D exchange. Such experiments were however not carried out so far.

Acknowledgment. This work was supported by a grant from GIF, the German–Israeli Foundation for Scientific Research and Development. We are grateful to Professor S. Alexander and A. Burshtein for useful discussion concerning the dynamic model.

Appendix

In this Appendix we describe a procedure to calculate the dynamic NMR line shape obtained by solving eq 5 of the main text. To do so we divide the range of φ into $2N + 1$ segments and write for each of the magnetizations $M_i(t)$ of the segment $\varphi_i - {}^1/_2\delta\varphi$ to $\varphi_i + {}^1/_2\delta\varphi$ a Bloch–McConnell type differential equation. The number of segments included in the calculation is limited to the range of φ outside which the equilibrium population $P^0(\varphi)$ is negligible (<1%). Each equation for M_i is coupled to its nearest neighbors M_{i-1} and M_{i+1} by the diffusion process viewed as infinitesimal jumps from and to the segments $\varphi_{i\pm1}$

$$\frac{dM_i(t)}{dt} = \left[-i\omega_Q^i - \frac{1}{T_2} - (k_{i+1,i} + k_{i-1,i})\right] M_i(t) + k_{i,i+1}M_{i+1}(t) + k_{i,i-1}M_{i-1}(t) \quad \text{(A1)}$$

where $\omega_Q^i \equiv \omega_Q(\Theta_i)$ is obtained from eq 6 by setting $\varphi = \varphi_i$, and the $k_{i,i\pm1}$ are rate constants for the jump diffusion from the segment $\varphi_{i\pm1}$ to the segment φ_i. These rate constants depend on the index i and are related to the diffusion constant D_R and the potential $V(\varphi)$ through the diffusion eq 3. To find the relation we expand the magnetization $M_{i+1}(t)$ in a Taylor series

$$M_{i+1}(t) = M_i(t) + \frac{\partial M_i(t)}{\partial\varphi}\delta\varphi + \frac{1}{2}\frac{\partial^2 M_i(t)}{\partial\varphi^2}(\delta\varphi)^2 + \ldots \quad \text{(A2)}$$

and substitute the series up to second order terms in eq A1 for $dM_i(t)/dt$

$$\frac{dM_i(t)}{dt} = \left[-i\omega_Q^i - \frac{1}{T_2}\right]M_i(t) - (k_{i+1,i} + k_{i-1,i})M_i(t) + k_{i,i+1}\left[M_i(t) + \frac{\partial M_i(t)}{\partial\varphi}\delta\varphi + \frac{1}{2}\frac{\partial^2 M_i(t)}{\partial\varphi^2}(\delta\varphi)^2\right] + k_{i,i-1}\left[M_i(t) - \frac{\partial M_i(t)}{\partial\varphi}\delta\varphi + \frac{1}{2}\frac{\partial^2 M_i(t)}{\partial\varphi^2}(\delta\varphi)^2\right] = \left[-i\omega_Q^i - \frac{1}{T_2}\right]M_i(t) + \left[\frac{1}{2}(k_{i,i+1} + k_{i,i-1})(\delta\varphi)^2\frac{\partial^2}{\partial\varphi^2} + (k_{i,i+1} - k_{i,i-1})\delta\varphi\frac{\partial}{\partial\varphi} + (k_{i,i+1} + k_{i,i-1} - k_{i+1,i} - k_{i-1,i})\right]M_i(t) \quad \text{(A3)}$$

On the other hand for $\varphi = \varphi_i$ ($m = 1$) eq 5 acquires the form (using the definitions in eqs 4 and 1)

$$\frac{dM_i(t)}{dt} = \left[-i\omega_Q^i - \frac{1}{T_2}\right]M_i(t) + D_R\left[\frac{\partial^2}{\partial\varphi^2} + 2V_0\beta\varphi_i\frac{\partial}{\partial\varphi} + 2V_0\beta\right]M_i(t) \quad (A4)$$

For eqs A3 and A4 to be equal for all values of φ we require that the coefficients of $\partial^n/\partial\varphi^n$ in both equations be identical, i.e.

$$D_R = {}^1/_2(k_{i,i+1} + k_{i,i-1})(\delta\varphi)^2 \quad (A5a)$$

$$2V_0\beta\varphi_i D_R = (k_{i,i+1} - k_{i,i-1})\delta\varphi \quad (A5b)$$

$$2V_0\beta D_R = k_{i,i+1} + k_{i,i-1} - k_{i+1,i} - k_{i-1,i} \quad (A5c)$$

which give the connections between the $k_{i,j}$'s and D_R. In addition we have the detailed balance relation

$$\frac{k_{i,i+1}}{k_{i+1,i}} = \frac{\exp(-\beta V_0\varphi_i^2)}{\exp(-\beta V_0\varphi_{i+1}^2)} = \exp\left[2\beta V_0(\delta\varphi)\left(\varphi_i + \frac{1}{2}\delta\varphi\right)\right] \quad (A6)$$

The four equations A5 and A6 are not independent and it is sufficient to consider just two of them to derive all rate constants for an assumed value of D_R. Thus by symmetry (or from eq A5b for $i = 0$) $k_{0,1} = k_{0,-1}$ so that from eq A5a

$$k_{0,\pm1} = \frac{D_R}{(\delta\varphi)^2} \quad (A7a)$$

and from eq A6

$$k_{\pm1,0} = k_{0,\pm1}\exp[-\beta V_0(\delta\varphi)^2] \quad (A7b)$$

Applying again eqs A5a and A6 we obtain

$$k_{\pm1,\pm2} = \frac{2D_R}{(\delta\varphi)^2} - k_{\pm1,0} \quad (A8a)$$

$$k_{\pm2,\pm1} = k_{\pm1,\pm2}\exp[-2\beta V_0(\delta\varphi)(\varphi_{\pm1} + {}^1/_2(\delta\varphi))] \quad (A8b)$$

By successive applications of these equations all desired k's can be computed for the whole set of $2N + 1$ segments, $-N < i < N$ (see Figure 5c).

The set of differential equations (A1) can be written in a compact matrix form

$$\frac{d}{dt}\mathbf{M}(t) = -R\mathbf{M}(t) \quad (A9)$$

where $\mathbf{M}(t)$ is a $(2N + 1)$-dimensional vector of the $M_i(t)$ and R is a $(2N + 1) \times (2N + 1)$-dimensional tridiagonal matrix with elements

$$R_{ii} = i\omega_Q^i + \frac{1}{T_2} + (k_{i+1,i} + k_{i-1,i}) \quad (A10a)$$

$$R_{i,j} = -k_{i,j}\delta_{j,i\pm1} \quad (A10b)$$

except that to account for the truncation at $\pm N$, $k_{\pm(N+1),\pm N}$ and $k_{\pm N,\pm(N+1)}$ were set equal to zero. Solution of eq A9 gives

$$\mathbf{M}(t) = \exp(-Rt)\,\mathbf{M}(0) \quad (A11)$$

where $\mathbf{M}(0)$ is the vector of the $M_i(0)$ which are proportional to the equilibrium populations, $P_i^0 = P^0(\varphi_i)$ (eq 2). In the quadrupole echo experiment, $(\pi/2)_{\pm x}$–τ–$(\pi/2)_y$–τ–(±)acquisition (t), the acquired FID signal is obtained by repeated application of eq A11, noting that the initial magnetization vector immediately after the $(\pi/2)_y$ pulse is the complex conjugate of its value just before the pulse, $\mathbf{M}(\tau)^+ = [\mathbf{M}(\tau)^-]^*$. The general solution is given in the literature[35] and will not be repeated here. The final result is

$$\mathrm{FID}(t) = Re\{\mathbf{1}T^{-1}\exp[-\Lambda(t+\tau)]T(T^{-1})^*\exp(-\Lambda^*\tau)T^*\mathbf{P}^0\} \quad (A12)$$

where $\Lambda = TRT^{-1}$ is a diagonal matrix of the eigenvalues of R, $\mathbf{1}$ is a $(2N + 1)$-dimensional vector with all elements unity, and P^0 is the column vector of the P_i^0's. The spectra that we have analyzed quantitatively were of unoriented powder samples. For the simulation we have therefore to isotropically average eq A12 over θ_0 and φ_0, followed by Fourier transformation, and reflecting the spectrum about zero frequency to account for the $m = -1$ transition. In practice 2584 θ_0,φ_0 pairs were used employing the Conroy–Wolfsberg sampling algorithm,[39] and the number of segments was 17 with $\delta\varphi$ values ranging from 4.1° to 10.6°, depending on the value of V_0.

(39) Conroy, H. *J. Chem. Phys.* **1967**, *47*, 5307. Cheng, V. B.; Suzukawa, H. H.; Wolfsberg, M. *J. Chem. Phys.* **1973**, *59*, 3992. Suzukawa, H. H.; Thompson, D. L.; Cheng, V. B.; Wolfsberg, M. *J. Chem. Phys.* **1973**, *50*, 4000.